A new class of electrolytes based on magnesium bis(diisopropyl)amide for magnesium-sulfur batteries

Xinghe Zhao, Yuanying Yang, Yanna NuLi,* Dongyu Li, Yurui Wang, Xuelin Xiang

Supporting Information

Preparation of electrolyte and sulfur@microporous composite

The preparation of electrolytes was conducted in an argon-filled glove box (Mbraun, Unilab, Germany) with H_2O and O_2 below 2 ppm. 0.25 mol L^{-1} MBA-$AlCl_3$/THF electrolytes with molar ratios of 2:1, 1:1 and 1:2 for MBA to $AlCl_3$ were prepared by dissolving the predetermined amount of magnesium bis(diisopropyl)amide (MBA, 0.7 mol L^{-1} solution in THF, Sigma-Aldrich, >99.5%) and $AlCl_3$ (Sigma-Aldrich, 99.99%) in tetrahydrofuran (THF) (Aladdin, further dried using a 3 Å molecular sieve) or THF and 1,3-dioxolane (DOL) (Aladdin, further dried using a 3 Å molecular sieve), THF and dimethoxyethane (DME) (Aladdin, further dried using a 3 Å molecular sieve), THF and tetraglyme (TG) (Aladdin, further dried using a 3 Å molecular sieve) mixed solvents (1:1 volume ratio) under stirring at room temperature for at least 4h. 0.4 mol L^{-1} $(PhMgCl)_2$+$AlCl_3$/THF electrolyte was obtained by dissolving the predetermined amount of PhMgCl (Sigma-Aldrich, 95%) and $AlCl_3$ in THF under stirring for at least 24h.

Sulfur@microporous carbon (S@MC) composite with 55.8 wt% sulfur content was prepared by a melt-diffusion method. Sublimed sulfur (S, 99.99%, Sigma-Aldrich) and commercial microporous carbon (MC, ACS Material LLC, USA) at a weight ratio of 4:1 were mixed by ball-milling at 350 rmp for 1h. Subsequently, the mixture was heated at 155 °C for 25h with a heating rate of 0.5 °C min^{-1}, then at 300 °C for 3h with a heating rate of 5°C min^{-1} in a tubular furnace under argon atmosphere, causing the molten sulfur to flow into the pores of the MC to achieve the S@MC composite.

Material Characterization

The ionic conductivity of the solutions was measured using a DDB-303A conductivity meter (INESA INSTRUMENT). X-ray diffraction (XRD) analysis of the magnesium deposits was conducted on a Rigaku diffractometer D/MAX-2200/PC equipped with Cu Kα radiation. The morphology of the deposits was observed using scanning electron microscopy (SEM) on a FEI SIRION200 field-emission microscope. Before the analysis of the deposits, the sample deposited for 50 hour at 0.088 mA cm^{-2} was washed in the argon-filled glove box with drying THF solvent to remove soluble residue and then transferred out of the box and kept without exposure to the atmosphere.

S@MC composite was characterized by XRD, thermogravimetric analysis (TGA) using a Thermo Gravimetric Analyzer (TGA/Pyris 1 TGA), X-ray Photoelectron Spectroscopy (XPS) analysis performed on an AXIS UltraDLD, SEM using a JEOL field-emission microscope (JSM-7401F) and transmission electron microscopy (TEM) performed on a JEOL high-resolution electron microscope (JEM-2010). After discharging to 0.5V, the cathodes were washed with drying THF solvent to remove soluble residue in the argon-filled glove box and then transferred out of the glove box without exposure to the atmosphere.

Electrochemical Measurements

Cyclic voltammograms (CVs) were conducted in three-electrode cells inside an argon-filled glove box using an electrochemical instrument of CHI604A Electrochemical Workstation (Shanghai, China). The working

electrode was a stainless steel, aluminum, copper and platinum disk (geometric area = 3.14×10^{-2} cm^2), which was polished with a corundum suspension and rinsed with dry acetone before use, and magnesium ribbon as counter and reference electrodes. Electrochemical magnesium plating/stripping cycles were examined with CR2016 experimental coin cells on a land battery measurement system (Wuhan, China). Stainless steel foil (Φ12 mm) was served as the working electrode (substrate). Mg ribbon as the counter electrode. An Entek PE and a fiber membrane as the separator. The cells were assembled in the argon-filled glove box. Magnesium was plated onto the stainless steel substrate for fixed periods of 30 min followed by stripping to a fixed potential limit of 0.8 V *vs*. Mg at a constant current density of 0.088 mA cm^{-2}. There was a 30 second rest between plating and stripping. The magnesium plating and stripping on the substrate were referred to as the discharge and charge process, respectively. The time of charge divided by the time of discharge was defined as the plating/stripping efficiency.

The S@MC electrode was prepared by casting and pressing an 8:1:1 weight-ratio mixture of S@MC, super-P carbon powder (timcal) and polyvinylidene fluoride (PVDF) binder dissolved in N-methyl-2-pyrrolidinone (NMP) onto copper current collector followed by drying in vacuum at 50 ^oC. CR2016 coin cells were fabricated with S@MC cathode, Mg anode, Entek PE and fiber membrane separator, and 0.25 mol L^{-1} MBA+2$AlCl_3$/THF or 0.4 mol L^{-1} $(PhMgCl)_2$+$AlCl_3$/THF electrolyte. LiCl (Alfa Aesar, ultra dry, 99.9%) with different concentrations was further added in the electrolytes to improve the electrochemical performance of the Mg-S batteries. The discharge-charge tests of the coin cells were carried out on a land battery measurement system (Wuhan, China) with the cutoff voltage of 0.5/1.7 V *vs*. Mg.

Table S1. Crystal data and structure refinement for $[Mg_2(\mu\text{-}Cl)_2(THF)_6](AlCl_4)_2$

Empirical formula	$C_{24}H_{48}O_6Mg_2A_{12}Cl_{10}$
Formula weight	889.74
Temperature/K	173
Crystal system	monoclinic
a/Å	10.814
b/Å	12.9032
c/Å	13.3989
α/°	63.042
β/°	90
γ/°	90
Volume/Å^3	1666.46
Z	33
ρ_{calc} mg/mm^3	1.552
m/mm^{-1}	0.766
F(000)	768.0
Crystal size/mm^3	0.12 × 0.13 × 0.13
2Θ range for data collection	3.70 to 68.53°
Index ranges	-12≤ h ≤ 12, -14 ≤ k ≤ 14, -14 ≤ l ≤ 14
Reflections collected	22891
Independent reflections	4566[R(int) = 0.0452，R(sigma) = 0.0389]
Data/restraints/parameters	4566/0/334
Goodness-of-fit on F2	2.615
Final R indexes [I>=2σ (I)]	R1 = 0.1521, wR2 =0.5012
Final R indexes [all data]	R1 = 0.1549, wR2 = 0.5012
Largest diff. peak/hole / e Å^{-3}	0.04/-0.77

Table S2. Fractional Atomic Coordinates (×104) and Equivalent Isotropic Displacement Parameters (Å2×103) for $[Mg_2(\mu\text{-}Cl)_2(THF)_6](AlCl_4)_2$. Ueq is defined as 1/3 of the trace of the orthogonalised UIJ tensor.

Atom	x	y	z	U(eq)
Al1	0.7511	0.3971	0.82684	0.0532
C0AA	1.0906	0.2764	0.194	0.069
C1	0.6885	0.4696	0.1866	0.06
C11	1.0573	0.1521	0.2133	0.063
C12	0.9623	0.1158	0.3034	0.057
C13	0.8416	0.2276	0.6136	0.082
C14	0.9587	0.208	0.6818	0.098
C15	1.0542	0.2523	0.5994	0.094
C16	1.0092	0.234	0.5022	0.065
C17	0.5273	0.1541	0.569	0.06
C18	0.4076	0.2125	0.5766	0.065
C19	0.4519	0.3323	0.558	0.069
C2	0.7279	0.5925	0.1352	0.072
C20	0.5493	0.3576	0.4698	0.068

C21	0.1763	-0.0007	0.9126	0.065
C22	0.1582	0.0307	1.0056	0.074
C23	0.2833	0.074	1.022	0.079
C24	0.3516	0.0908	0.9143	0.086
C3	0.757	0.6112	0.238	0.069
C4	0.8142	0.4974	0.3172	0.0537
C5	0.6578	0.1668	0.2043	0.07
C6	0.5399	0.1512	0.1551	0.095
C7	0.4438	0.2089	0.1865	0.093
C8	0.4907	0.2103	0.2901	0.063
C9	0.9666	0.3204	0.2103	0.062
Cl1	0.7881	0.5171	0.6571	0.1011
Cl2	0.6483	0.2537	0.8299	0.0766
Cl3	0.6497	0.478	0.9079	0.1011
Cl4	0.9228	0.3352	0.913	0.0753
Cl5	0.75179	0.00618	0.51333	0.02
H0AA	1.1519	0.2751	0.2493	0.082
H0AB	1.1229	0.324	0.1174	0.082
H11A	1.023	0.1525	0.1446	0.076
H11B	1.1303	0.1002	0.2381	0.076
H12A	0.9007	0.0638	0.2946	0.068
H12B	1.0016	0.074	0.3779	0.068
H13A	0.7885	0.1575	0.6472	0.098
H13B	0.7947	0.294	0.6126	0.098
H14A	0.9559	0.2509	0.7272	0.117
H14B	0.9713	0.1243	0.7322	0.117
H15A	1.1325	0.2098	0.6293	0.113
H15B	1.0682	0.336	0.576	0.113
H16A	1.0462	0.2914	0.4309	0.078
H16B	1.0288	0.1546	0.5131	0.078
H17A	0.5713	0.1193	0.6416	0.073
H17B	0.511	0.0929	0.5454	0.073
H18A	0.3684	0.1694	0.6511	0.078
H18B	0.3481	0.2186	0.518	0.078
H19A	0.3842	0.3903	0.5306	0.083
H19B	0.4873	0.3298	0.6272	0.083
H1A	0.5977	0.464	0.1969	0.073
H1B	0.7118	0.4335	0.138	0.073
H20A	0.5125	0.4002	0.3942	0.081
H20B	0.6157	0.4061	0.4778	0.081
H21	0.1349	-0.0599	0.902	0.079
H22A	0.1318	-0.038	1.0748	0.089
H22B	0.0948	0.0923	0.9856	0.089
H23A	0.3253	0.0158	1.0901	0.095

H23B	0.2759	0.1482	1.0266	0.095
H24	0.4369	0.1084	0.899	0.103
H2A	0.6608	0.6448	0.0897	0.086
H2B	0.802	0.6053	0.0877	0.086
H3A	0.8156	0.6764	0.2191	0.082
H3B	0.6808	0.6267	0.27	0.082
H4A	0.904	0.4974	0.3029	0.064
H4B	0.8017	0.4823	0.3958	0.064
H5A	0.72	0.075	0.285	0.084
H5B	0.746	0.208	0.173	0.025
H6A	0.5468	0.186	0.0725	0.114
H6B	0.5206	0.0675	0.1843	0.114
H7A	0.3649	0.1655	0.2011	0.112
H7B	0.4304	0.289	0.1267	0.112
H8A	0.4434	0.2083	0.3507	0.075
H8B	0.463	0.286	0.29	0.019
H9A	0.9779	0.3807	0.2359	0.075
H9B	0.9198	0.3548	0.1391	0.075
Mg1	0.75092	0.22479	0.39502	0.0389
O1	0.7508	0.4103	0.295	0.0493
O2	0.6234	0.2153	0.279	0.0452
O3	0.9021	0.2239	0.2921	0.0439
O4	0.8748	0.251	0.5038	0.0474
O5	0.5981	0.2499	0.484	0.0476
O6	0.2675	0.0756	0.8441	0.0795

Table S3. Fractional Atomic Coordinates (×104) and Equivalent Isotropic Displacement Parameters (Å2×103) for $[Mg_2(\mu\text{-}Cl)_2(THF)_6](AlCl_4)_2$. Ueq is defined as 1/3 of the trace of the orthogonalised UIJ tensor.

Atom	U11	U22	U33	U12	U13	U23
Al1	0.000547134	0.000833367	0.000606661	-0.0000355	-0.0000418	-0.000295098
C0AA	0.000671253	0.00119052	0.000987882	-0.000113986	-0.00113986	-0.000709248
C1	0.000683918	0.000772574	0.000772574	-0.0000126651	-0.000126651	-0.000291298
C11	0.000645923	0.00115253	0.000658588	0.000088656	0.00088656	-0.000455945
C12	0.000531936	0.0008359	0.00086123	0.000164647	0.00164647	-0.00044328
C13	0.000671253	0.00181112	0.000759909	0.0000506606	0.000506606	-0.000696583
C14	0.000899226	0.00210241	0.000911891	0.000215308	0.00215308	-0.00086123
C15	0.000671253	0.00220374	0.000911891	-0.000113986	-0.00113986	-0.000899226
C16	0.000506606	0.00132984	0.000671253	0.0000253303	0.000253303	-0.000506606
C17	0.000645923	0.000899226	0.000747244	0	0	-0.0000367289
C18	0.000633257	0.000962551	0.000848565	0.0000633257	0.000633257	-0.000354624
C19	0.000734579	0.00116519	0.000899226	0.000189977	0.00189977	-0.000620592
C2	0.000873895	0.000949886	0.000759909	0.000164647	0.00164647	-0.000253303
C20	0.000759909	0.000899226	0.00107654	0.000088656	0.00088656	-0.000582597
C21	0.000582597	0.00111453	0.000772574	-0.000113986	-0.00113986	-0.00041795

C22	0.000683918	0.00121585	0.00115253	-0.000088656	-0.00088656	-0.000721913
C23	0.000797904	0.000962551	0.00124118	-0.000151982	-0.00151982	-0.000493941
C24	0.000747244	0.00100055	0.00157048	-0.000177312	-0.00177312	-0.000620592
C3	0.000848565	0.0008359	0.00105121	-0.0000633257	-0.000633257	-0.000531936
C4	0.000607927	0.000759909	0.000721913	-0.000126651	-0.00126651	-0.000379954
C5	0.000671253	0.00129185	0.000987882	0.0000379954	0.000379954	-0.000772574
C6	0.000911891	0.00197576	0.00115253	-0.000088656	-0.00088656	-0.00107654
C7	0.000734579	0.00203909	0.00130451	0.0000759909	0.000759909	-0.00122852
C8	0.000582597	0.00116519	0.0008359	-0.000101321	-0.00101321	-0.000633257
C9	0.000671253	0.000911891	0.000899226	0.0000253303	0.000253303	-0.000493941
Cl1	0.00148182	0.00118292	0.000683918	-0.000371089	-0.00371089	0.00000633
Cl2	0.000928355	0.0011348	0.000882761	-0.000401485	-0.00401485	-0.000487608
Cl3	0.000976483	0.00169713	0.00157048	0.000340692	0.00340692	-0.00110187
Cl4	0.000661121	0.00123738	0.000827034	0.000044328	0.00044328	-0.000347025
Cl5	0.000149449	0.000234305	0.000311563	0.0000240638	0.000240638	-6.71E-05

H0AA	0.0126651	0.0126651	0.0126651	0.0126651	0.126651	0.0126651
H0AB	0.0126651	0.0126651	0.0126651	0.0126651	0.126651	0.0126651
H11A	0.0126651	0.0126651	0.0126651	0.0126651	0.126651	0.0126651
H11B	0.0126651	0.0126651	0.0126651	0.0126651	0.126651	0.0126651
H12A	0.0126651	0.0126651	0.0126651	0.0126651	0.126651	0.0126651
H12B	0.0126651	0.0126651	0.0126651	0.0126651	0.126651	0.0126651
H13A	0.0126651	0.0126651	0.0126651	0.0126651	0.126651	0.0126651
H13B	0.0126651	0.0126651	0.0126651	0.0126651	0.126651	0.0126651
H14A	0.0126651	0.0126651	0.0126651	0.0126651	0.126651	0.0126651
H14B	0.0126651	0.0126651	0.0126651	0.0126651	0.126651	0.0126651
H15A	0.0126651	0.0126651	0.0126651	0.0126651	0.126651	0.0126651
H15B	0.0126651	0.0126651	0.0126651	0.0126651	0.126651	0.0126651
H16A	0.0126651	0.0126651	0.0126651	0.126651	0.126651	0.0126651
H16B	0.0126651	0.0126651	0.0126651	0.126651	0.126651	0.0126651
H17A	0.0126651	0.0126651	0.0126651	0.126651	0.126651	0.0126651
H17B	0.0126651	0.0126651	0.0126651	0.126651	0.126651	0.0126651
H18A	0.0126651	0.0126651	0.0126651	0.126651	0.126651	0.0126651
H18B	0.0126651	0.0126651	0.0126651	0.126651	0.126651	0.0126651
H19A	0.0126651	0.0126651	0.0126651	0.126651	0.126651	0.0126651
H19B	0.0126651	0.0126651	0.0126651	0.126651	0.126651	0.0126651
H1A	0.0126651	0.0126651	0.0126651	0.126651	0.126651	0.0126651
H1B	0.0126651	0.0126651	0.0126651	0.126651	0.126651	0.0126651
H20A	0.0126651	0.0126651	0.0126651	0.126651	0.126651	0.0126651
H20B	0.0126651	0.0126651	0.0126651	0.126651	0.126651	0.0126651
H21	0.0126651	0.0126651	0.0126651	0.126651	0.126651	0.0126651
H22A	0.0126651	0.0126651	0.0126651	0.126651	0.126651	0.0126651
H22B	0.0126651	0.0126651	0.0126651	0.126651	0.126651	0.0126651
H23A	0.0126651	0.0126651	0.0126651	0.126651	0.126651	0.0126651
H23B	0.0126651	0.0126651	0.0126651	0.126651	0.126651	0.0126651

H24	0.0126651	0.0126651	0.0126651	0.126651	0.126651	0.0126651
H2A	0.0126651	0.0126651	0.0126651	0.126651	0.126651	0.0126651
H2B	0.0126651	0.0126651	0.0126651	0.126651	0.126651	0.0126651
H3A	0.0126651	0.0126651	0.0126651	0.126651	0.126651	0.0126651
H3B	0.0126651	0.0126651	0.0126651	0.126651	0.126651	0.0126651
H4A	0.0126651	0.0126651	0.0126651	0.126651	0.126651	0.0126651
H4B	0.0126651	0.0126651	0.0126651	0.126651	0.126651	0.0126651
H5A	0.0126651	0.0126651	0.0126651	0.126651	0.126651	0.0126651
H5B	0.0126651	0.0126651	0.0126651	0.126651	0.126651	0.0126651
H6A	0.0126651	0.0126651	0.0126651	0.126651	0.126651	0.0126651
H6B	0.0126651	0.0126651	0.0126651	0.126651	0.126651	0.0126651
H7A	0.0126651	0.0126651	0.0126651	0.126651	0.126651	0.0126651
H7B	0.0126651	0.0126651	0.0126651	0.126651	0.126651	0.0126651
H8A	0.0126651	0.0126651	0.0126651	0.126651	0.126651	0.0126651
H8B	0.0126651	0.0126651	0.0126651	0.126651	0.126651	0.0126651
H9A	0.0126651	0.0126651	0.0126651	0.126651	0.126651	0.0126651
H9B	0.0126651	0.0126651	0.0126651	0.126651	0.126651	0.0126651
Mg1	0.000405285	0.000577531	0.000509139	0.000151982	0.000151982	-0.000259636
O1	0.000645923	0.000582597	0.000595262	0.000544601	0.000544601	-0.000215308
O2	0.000531936	0.000620592	0.000582597	0.000164647	0.000164647	-0.000291298
O3	0.00046861	0.000633257	0.000607927	0.000189977	0.000189977	-0.000316629
O4	0.000544601	0.000759909	0.000569932	-0.000379954	-0.000379954	-0.000367289
O5	0.000519271	0.000658588	0.000595262	0.000455945	0.000455945	-0.000265968
O6	0.000975216	0.0010892	0.000785239	-0.000633257	-0.000633257	-0.000278633

Table S4. Comparison of cycling performance of Mg-S batteries reported in the literatures with this work.

Cathode material	S content (wt%)	Electrolyte		Cycling performance			Ref.
				Current density (C, mA g^{-1}_S)	Discharge plateau (V *vs*. Mg)	Final discharge capacity (mAh g^{-1}_S)/cycle number	
S/CMK-3	55	1.2 mol L^{-1} $(HMDS)_2Mg+(AlCl_3)_2+MgCl_2$/PP14TFSI+diglyme	PVDF	20 mA g^{-1} （0.012 C）	1.65	about 150/20	5
			CMC		1.65	about 200/20	
		1.2 mol L^{-1} $(HMDS)_2Mg+(AlCl_3)_2+MgCl_2$/PP14TFSI +tetraglyme	PVDF		1.6	about 250/20	
			CMC		1.65	about 260/20	
S/rGO	49	1.8 mol L^{-1} $(HMDS)_2Mg+(AlCl_3)_2+MgCl_2$/tetraglyme		20 mA g^{-1} (0.012 C)	1.3~1.72 0.7-1.3	219/50	6
S/ACC	15	0.1 mol L^{-1} (HMDS)2Mg+ $(AlCl_3)_2$ + 1.0 mol L^{-1} LiTFSI/tetraglyme		1 C	1.75 1.2	1000/30	17
S/CNF	50	3.6 mol L^{-1} $(HMDS)_2Mg+(AlCl_3)_2+MgCl_2$/tetraglyme		0.02 C	about 1.55 0.85	about 750/20	7
S/C	85	0.5 mol L^{-1} THFPB+0.05 mol L^{-1} MgF_2/DME		50 mA g^{-1} (0.03 C)	1.05	about 980/30	9
S/C	/	0.5 mol L^{-1} THFPB+0.05 mol L^{-1} MgO/DME		10 mA g^{-1} (0.006 C)	1.1	1030/15	10
S/CMK-3	55	0.4 mol $L^{-1}Mg[B(hfip)_4]_2$/DME		0.1 C	1.25~1.5	200/100	11
S/CMK-3	69.3	0.3 mol L^{-1} $Mg(TFSI)_2$/glyme+diglyme		0.01 C	0.2	500/1	13
S/ACC	/	0.25 mol L^{-1} $MgTFSI_2+MgCl_2$/DME		200 mA g^{-1} (0.12 C)	1.25~1.5	about 410/20	14
		1.0 mol L^{-1} $MgTFSI_2+MgCl_2$/DME		100 mA g^{-1} (0.06 C)	1~1.25	about 600/110	
S@MC	55.8	0.4 mol L^{-1} $(PhMgCl)_2+AlCl_3$+1.0 mol L^{-1} LiCl/THF		0.04 C	1.1	270/100	This work
		0.25 mol L^{-1} BMA+2$AlCl_3$+1.0 mol L^{-1} LiCl /THF		0.04 C	1.1	400/100	

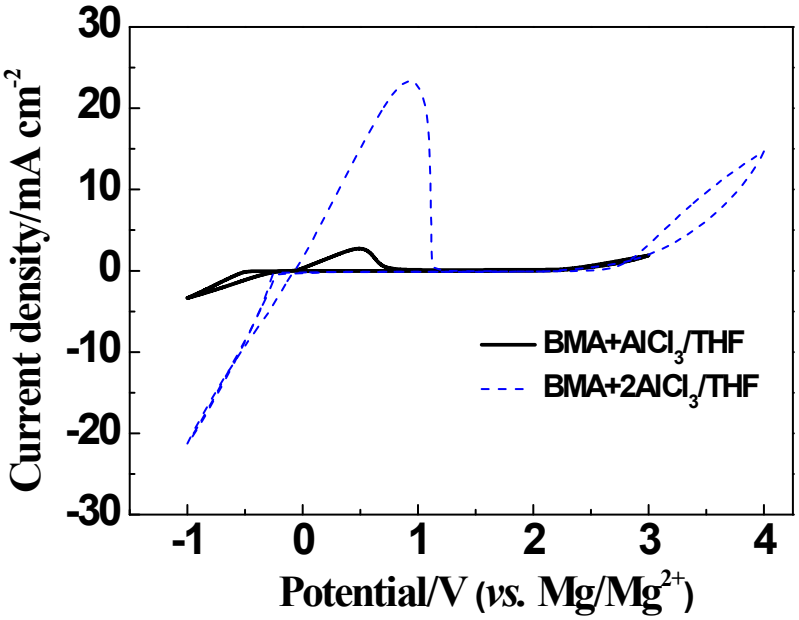

Figure S1. Comparison of CVs at 50 mV s^{-1} for Mg electrochemical plating/stripping on SS disk electrode in 0.25 mol L^{-1} MBA-$AlCl_3$/THF electrolytes with 1:1 and 1:2 molar ratios of MBA to $AlCl_3$.

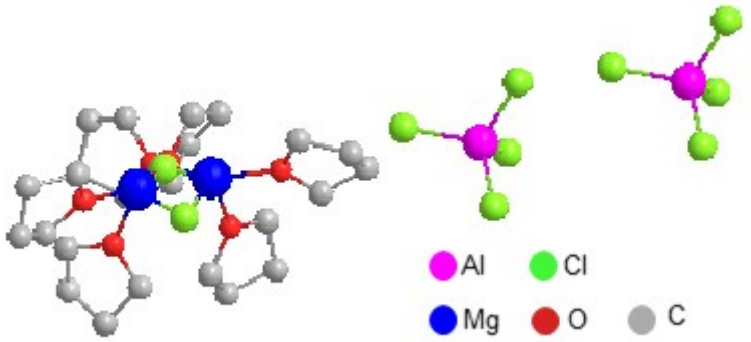

Figure S2. Molecular structures of $[Mg_2(\mu\text{-}Cl)_2(THF)_6]^{2+}[AlCl_4]_2^-$. Hydrogen atoms are omitted for clarity.

The asymmetric unit consists of an ionic pair. The cationic species has a typical structure of dimeric magnesium bridged by three chlorine atoms and each magnesium atom being solvated by three THF molecules. The counter anion is an aluminum atom tetrahedrally coordinated by four chlorine atom. Based on the data of single-crystal XRD, we suppose that the reaction between MBA and $AlCl_3$ at the 1:2 molar ratio is represented as equation (1):

$$2Mg[N(C_3H_7)_2]_2 + 4AlCl_3 \xrightarrow{THF} [Mg_2(\mu\text{-}Cl)_2(THF)_6]^{2+}[AlCl_4]_2^- + 2[N(C_3H_7)_2]_2AlCl \quad (1)$$

The aluminate anion can be stabilized by the electron donating effect of $(C_3H_7)_2N$ ligand, which is also beneficial to the electrochemical stability

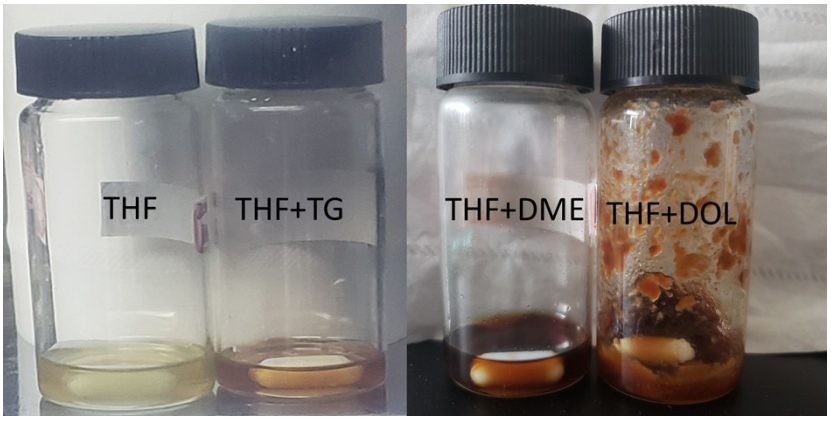

Figure S3. The photo of 0.25 mol L^{-1} BMA+2$AlCl_3$ solutions with THF, THF+TG (1:1 volume ratio), THF+DME (1:1 volume ratio) and THF+DOL (1:1 volume ratio) solvents.

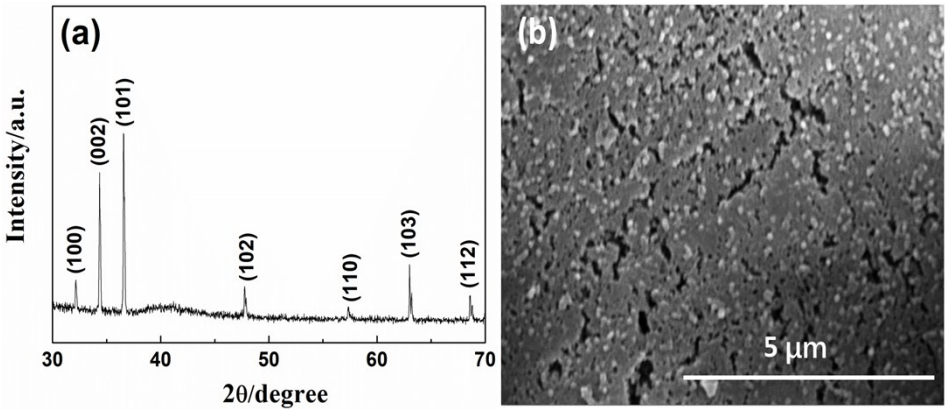

Figure S4. X-ray diffraction result (a) and SEM image (b) of electrodeposits from 0.25 mol L^{-1} BMA+2$AlCl_3$/THF solution. The deposits were obtained at 15.84 C cm^{-2} charge.

As shown in Fig. S4a, the diffraction peaks observed at 2θ = 32.2°, 34.4°, 36.6°, 47.8°, 57.4°, 63.1° and 68.6° are in good accordance with the (100), (002), (101), (102), (110), (103) and (112) diffractions of metallic Mg (JCPDS file 35-0821), respectively. No other phases are identified, suggesting that deposition of pure metallic magnesium has been successfully obtained from the solution and confirming the crystalline metallic nature of these magnesium deposits. SEM image in Fig. S4b exhibits that the deposition layer obtained at 15.84 C cm^{-2} charge (at a constant current density of 0.088 mA cm^{-2} for 50 hours) is compact and uniform, which is very important for practical uses. The magnesium deposits appear in an agglomerated particles with an average size of from ca. 100 to 300 nm, evenly spread over the surface.

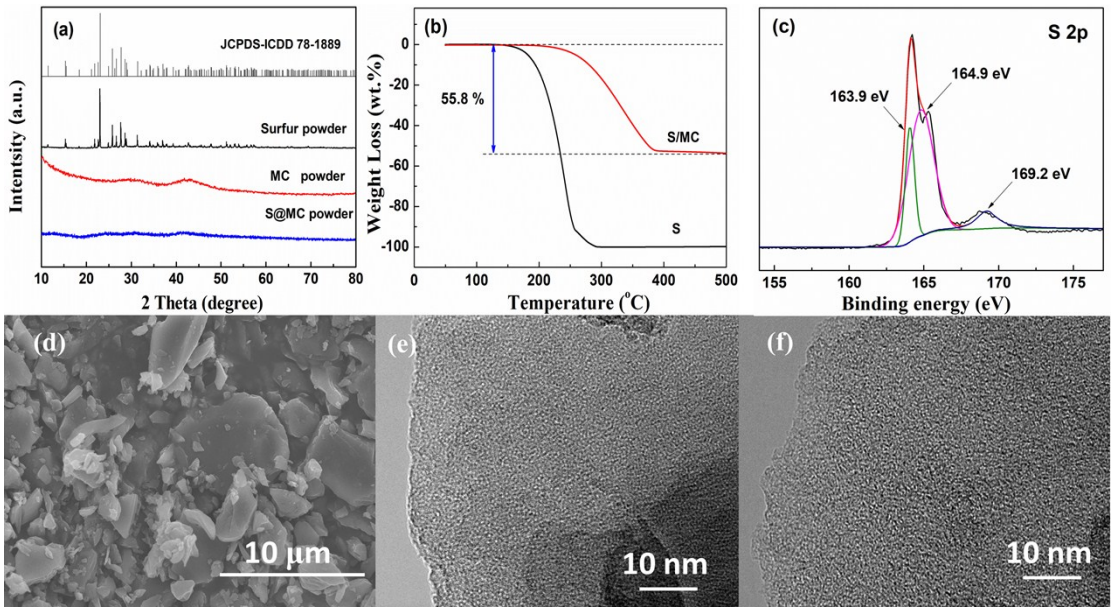

Figure S5. XRD results of S powder, MC powder, S@MC composite powder (a). TGA curves of S and S@MC composite (b). The high resolution S 2p XPS spectra of S@MC powder (c). SEM images of MC (d) and S@MC composite (e). TEM image of S@MC composite (f).

X-ray diffraction (XRD) patterns in Fig. S5a show that the sharp diffraction peaks of bulk crystalline sulfur disappear entirely after encapsulating sulfur into the micropores of carbon, demonstrating that sulfur exists as a highly dispersed state inside the micropores of carbon. All sulfur content in the S@MC composite is calculated to be 55.8 wt% according to the weight loss (Fig. S5b). The peaks at 163.9 and 164.9 eV in X-ray photoelectron spectroscopy (XPS) result (Fig. S5c) can be attributed to $S2p_{3/2}$ and S $2p_{1/2}$ of the sulfur species containing S-S bond, probably arising from short-chain S_x (x< 8).[1] Furthermore, the additional peak at a higher binding energy of 169.2 eV arises from sulfur atoms located at the chain end of small S_{2-4} molecules.[2] Scanning electron microscopy (SEM) image demonstrates that S@MC composite is composed of bitty patches with sizes about 1-10 μm (Fig. S5d). The filling of the microporous carbon with sulfur is corroborated by the undistinguishable difference of transmission electron microscopy (TEM) images for MC and S@MC (Fig. S5e and Fig. S5f), confirming the highly dispersed sulfur inside the narrow micropores.

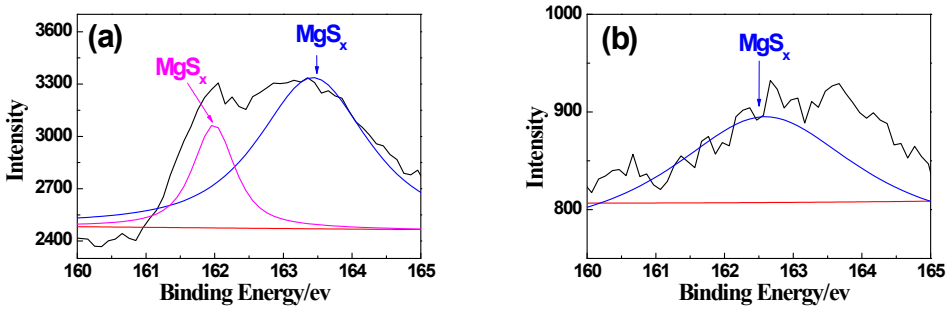

Figure S6. Comparison of surface XPS measurements of S@MC cathodes cycled in 0.25 mol L^{-1} BMA+2$AlCl_3$/THF electrolyte in the absence (a) and presence (b) of LiCl.

The XPS result for the cathode from the electrolyte without LiCl shows that S $2p_{3/2}$ peaks appear at 163.5 and 162.0 eV, which are assigned to the Mg-S bonds in magnesium polysulfides (MgS_x, $1<x<8$),[3] as shown in Fig. S6a. When LiCl is added (Fig. S6b), slightly reduced peak (163.5 eV) shifts to a lower value (162.5 eV) and highly reduced peak (162.0 eV) disappears, indicating that the decrease of magnesium polysulfides in electrolyte with LiCl additive.

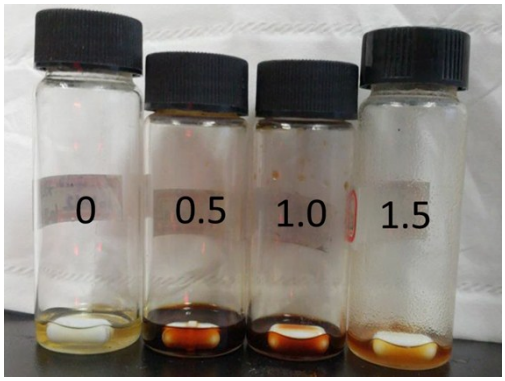

Figure S7. The photo of 0.25 mol L^{-1} BMA+2$AlCl_3$/THF solutions containing LiCl at different concentrations.

References

1. C. Luo, Y. J. Zhu, O. Borodin, T. Gao, X. L. Fan, Y. H. Xu, K. Xu, C. S. Wang, Adv. Funct. Mater. 2016, 26, 745−752.
2. Z. Li, L. X. Yuan, Z. Q. Yi, Y. M. Sun, Y. Liu, Y. Jiang, Y. Shen, Y. Xin, Z. L. Zhang, Y. H Huang, *Adv. Energy Mater.*, 2014, **4**, 1301473.
3. H. S. Kim, T. S. Arthur, G. D. Allred, J. Zajicek, J. G. Newman, A. E. Rodnyansky, A. G. Oliver, W. C. Boggess and J. Muldoon, *Nature Commun.*, 2011, **2**, 427.